

CHAPTER 1

Introduction and Literature Survey

1.1 Introduction

Hydrogen peroxide (H_2O_2) is a powerful green oxidizing agent widely used for chemical synthesis, pulp bleaching, cleaning, and disinfection [1]. It is also an environmentally friendly oxidant, with water and oxygen as the only by-products. Furthermore, H_2O_2 is widely used in fuel cells due to its high energy density and relatively safe storage [2,3]. Its advantages over traditional gaseous energy carriers, such as hydrogen, in terms of ease of storage and transportation, highlight its role as an efficacious clean fuel. H_2O_2 also finds extensive use in many industries for effluent treatment, particularly in processes such as Fenton, photo-Fenton, and electrochemical reactions for wastewater treatment [4–7].

The industrial production of H_2O_2 is primarily achieved through the multistep anthraquinone oxidation process. However, this process generates enormous quantities of hazardous waste and demands significant amounts of energy and chemicals [8]. Additionally, the transportation of large volumes of H_2O_2 poses risks and incurs considerable expenses, necessitating alternative solutions. One such alternative is the in situ production of H_2O_2 . This approach involves coupling the production reaction of H_2O_2 directly to its utilization, thereby eliminating the risks, energy demands, and costs associated with transportation. Moreover, in situ production would circumvent the need for the costly separation of H_2O_2 from other reactants, as required in the anthraquinone process [9]. A way forward in this direction for in situ production is the direct synthesis of H_2O_2 through a single-step reaction between H_2 and O_2 over a suitable catalyst. Catalysts such as Pd, Au-Pd bimetallic, and other metal nanocatalysts have been extensively studied for this reaction [10,11]. However, the explosive nature of H_2 and O_2 mixtures over an extended concentration range presents significant safety concerns. To mitigate these risks, large

amounts of N_2 are typically added to the reaction, but this safety measure significantly reduces H_2O_2 production efficiency.

The photocatalytic generation of H_2O_2 is a safer, greener, and economical method that would only require sunlight and an efficient photocatalyst in water. Photocatalysis involves the use of a photocatalyst, a material capable of absorbing light and catalyzing chemical reactions. When a photocatalyst is illuminated by electromagnetic radiation in the ultraviolet (UV) or visible spectrum, with energy equal to or greater than its bandgap, photoexcited electrons (e^-) are promoted from the valence band (VB) to the conduction band (CB). This transition leaves behind positively charged holes (h^+) in the VB. Photocatalysts that get excited by visible light can utilize a larger spectrum of solar electromagnetic radiation. After excitation, the excited species can recombine or react with chemical species with suitable redox potentials [1,12]. Based on the nature of the catalyst, photocatalysis can be categorized into two main types: homogeneous and heterogeneous photocatalysis.

Homogeneous photocatalysis involves photocatalyst in the same phase as the reactants, typically dissolved in a solution. The notable activity of homogeneous photocatalysts arises from their molecular-level dispersion within the reaction medium [13]. However, the primary drawback of homogeneous photocatalysis lies in the difficulty of separating the catalyst from the reaction mixture after the target reaction is complete. Catalyst separation is crucial for reuse and sustainability. In contrast, heterogeneous photocatalysis involves solid powder catalyst particles dispersed in a liquid reaction medium, allowing separation and recycling of the catalyst after use [14]. Consequently, this thesis focuses on the development of heterogeneous photocatalysts.

Heterogeneous photocatalysis was first demonstrated by Fujishima and Honda in 1972 during their study of water splitting using a photoelectrochemical cell with a single-

crystal TiO₂ electrode [15]. Since then, heterogeneous photocatalysts have been widely used in various applications, such as the production of H₂O₂ [16], detoxification of wastewater [17], CO₂ reduction [18], H₂ production [19], NH₃ synthesis [20], and organic transformations [21]. Semiconductor materials with suitable bandgap energies in the ultraviolet (UV) or visible range of the solar spectrum have been employed as heterogeneous photocatalysts. However, single-phase/component photocatalysts often suffer from several limitations.

- i) Limited absorption of visible light is a significant challenge for single-component photocatalysts. Solar radiation comprises approximately 44% visible light and only about 5% ultraviolet (UV) light. Photocatalysts with wide band gaps fail to efficiently absorb visible light, as their bandgap energies are not aligned with the visible region of the solar spectrum.
- ii) Inefficient separation of photogenerated charge carriers is a critical problem of single-component photocatalysts. Upon light absorption, the photocatalyst generates electron-hole pairs (e^- and h^+), which are highly reactive but extremely unstable. Due to their opposite charges, these carriers tend to recombine rapidly, releasing the absorbed energy as heat or light rather than driving catalytic reactions. The lifetimes of photo-excited charges (h^+ and e^-) are very short with these photocatalysts, resulting in reduced photocatalytic activity. Figure 1.1a provides a schematic illustration of the processes occurring within a single photocatalyst during a photocatalytic reaction.
- iii) Limited oxidation and reduction capability: Photocatalysts with a narrow or moderate bandgap may be ineffective for certain redox reactions due to the restricted positions of their VB and CB relative to the target reactants.

- iv) Adsorption Properties: The efficiency of a photocatalyst is significantly influenced by its ability to interact favorably with reactant species on its surface. Proper adsorption behavior facilitates the reduction or oxidation of reactants, thereby enhancing the overall photocatalytic performance.

There are several approaches to addressing these issues. One approach involves developing composites or heterostructures from two photocatalytic components, each with distinct roles. One component typically serves as the electron donor (reducing), while the other facilitates electron acceptance (oxidizing). Another effective method is the incorporation of plasmonic metals-semiconductor photocatalysts.

1.2 Composite/heterostructure photocatalysts

Composites or heterostructure photocatalysts are developed by forming interfaces between two or more semiconductors with specific band alignments to facilitate efficient charge carrier transfer and provide distinct adsorption properties for reactants. Achieving high photocatalytic activity in such systems involves addressing two key challenges: optimizing the bandgap of each semiconductor component to enhance solar light harvesting, particularly in the visible region, and minimizing the recombination of photogenerated electron-hole pairs. Heterojunctions play a pivotal role by creating energy offsets in the CB and/or VB edges, facilitating efficient separation of photoexcited electron-hole pairs. This separation promotes effective charge transfer across the interface in the junction region, ultimately enhancing photocatalytic performance [22,23].

Based on the bandgap and electronic energy levels of semiconductors, semiconductor heterojunctions can generally be classified into three main types: straddling alignment (Type I), staggered alignment (Type II, which includes Z-scheme systems and

p-n heterojunctions), and broken gap alignment (Type III). Conventional heterojunction photocatalysts typically fall into one of these categories depending on the relative positions of the conduction and valence bands of the constituent semiconductors [24,25]. The band gap, electron affinity (representing the lowest potential of the conduction band), and work function (indicating the highest potential of the valence band) of the combined semiconductors collectively determine the dynamics of electron and hole transfer in semiconductor heterojunctions [26].

1.2.1 Type-I (straddling alignment) and Type-III (broken gap) heterostructure photocatalyst

In a Type-I band alignment, the VB and CB edges of semiconductor II are entirely enclosed within the energy gap of semiconductor I, resulting in a straddling band configuration [27], as shown in Figure 1.1b. The VB and CB potentials of two distinct semiconductors are critical in determining the behavior of photogenerated charges and their influence on photocatalytic performance. The localization of both electrons and holes in the same semiconductor photocatalyst component often leads to recombination, reducing photocatalytic efficiency. This alignment might constrain the redox capabilities due to the limited separation of charge carriers between the semiconductors. Similarly, Type-III (broken gap) heterojunctions are where the band gaps of the two semiconductors do not overlap at all (Figure 1.1c). This misalignment prevents effective separation and migration of electron-hole pairs, making them unsuitable for promoting charge carrier separation.

Due to these limitations, Type I and Type III heterostructures are generally less suitable for photocatalytic applications. In contrast, staggered alignment (type-II), such as p-n heterojunctions and Z-scheme systems, is often preferred because of their superior

charge separation capabilities and favorable redox potential, which significantly enhances photocatalytic performance.

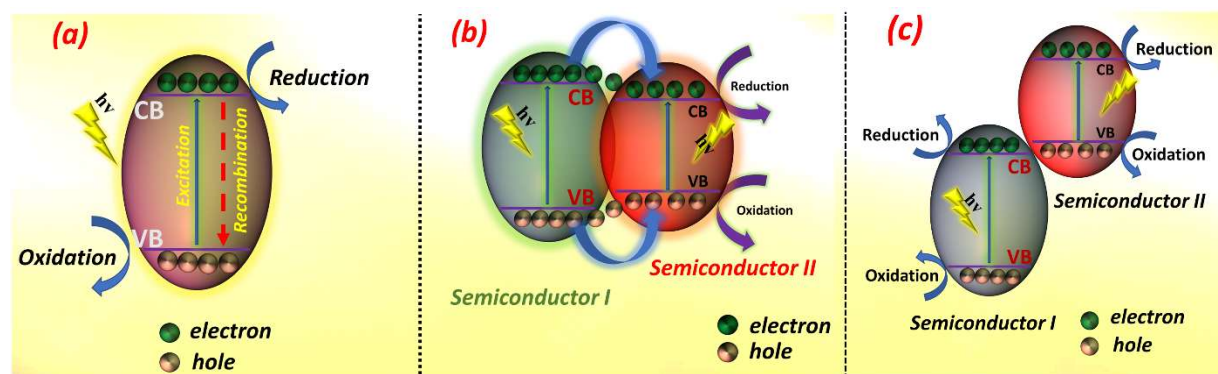


Figure 1.1 Schematic diagram of the (a) single-component semiconductor photocatalysis, (b) Type I heterostructure (straddling type), (c) Type III (broken gap) alignments.

1.2.2 Type-II Heterostructures (Staggered band alignment)

In a type-II heterostructure band alignment, the CB and VB of semiconductor 1 are both positioned higher than those of semiconductor 2. The band bending at the heterojunction interface, caused by the difference in chemical potential between semiconductors 1 and 2, generates a built-in electric field. This field facilitates the movement of photoexcited electrons and holes in opposite directions, effectively separating electron-hole pairs spatially across the heterojunction before recombination occurs. Moreover, intimate interfacial contact between the two components ensures smooth charge transfer across the junction, thereby minimizing interfacial resistance and energy loss. When coupled with a well-engineered nanostructure possessing a high surface area, the system exposes more active sites and shortens carrier diffusion pathways, allowing charge carriers to reach catalytic sites efficiently. Additionally, the synergistic integration of semiconductors with complementary optical and electronic properties extends light

absorption and enhances redox potential, ultimately maximizing the utilization of photogenerated carriers.

Generally, photocatalyst heterostructures with such staggered band alignments can be classified into two categories: (i) p-n heterojunctions and (ii) Z-scheme composite photocatalysts. Figure 1.2 illustrates the electron transfer mechanisms in these two distinct types of composite photocatalysts.

1.2.2.1 p-n heterojunction photocatalysts

The design of p-n heterostructure photocatalyst systems consisting of p-type and n-type semiconductors is one of the most common methods to improve the efficiency of photocatalytic reactions (Figure 1.2a). When the two semiconductors form a heterojunction, excess electrons on the n-type semiconductor and holes on the p-type semiconductor migrate toward the p-n interface [27]. This migration continues until the Fermi level equilibrium is reached, resulting in the development of an internal electric field at the interface. Upon irradiation with light of energy greater than the band gaps of the individual semiconductors, electron-hole pairs are generated. The photoexcited electrons in the more negative CB of the p-type semiconductor transfer to the relatively positive CB of the n-type semiconductor. Similarly, holes migrate from the more positive VB of the n-type semiconductor to the less positive VB of the p-type semiconductor. Consequently, electrons accumulate in the less negative CB, while holes concentrate in the more positive VB, leading to more effective electron-hole pair separation and an extended carrier lifetime. These properties significantly enhance the photocatalytic performance of p-n heterostructures. For instance, He et al. developed a novel $\text{CoFe}_2\text{O}_4/\text{g-C}_3\text{N}_4$ p-n heterojunction photocatalyst. The formation of the p-n heterojunction induced an internal

electric field at the interface, which significantly promoted the transfer of photogenerated charge carriers through a conventional p-n heterojunction mechanism between CoFe_2O_4 and $\text{g-C}_3\text{N}_4$ [28].

1.2.2.2 Z-scheme photocatalysts

In contrast, Z-scheme photocatalysts, upon irradiation with light energy equal to or greater than the bandgap of the constituent semiconductors, generate photoexcited electrons and holes in both components of the composite. As illustrated in Figure 1.2b, the photoexcited electrons in the CB of one semiconductor recombine with the holes in the valence band (VB) of the other. Ultimately, this process leads to the accumulation of oxidative holes in the more positive VB of one semiconductor and highly reductive electrons in the more negative CB of the other [27,29]. This charge distribution enhances the redox potential of the photocatalyst, as the hole-rich VB exhibits higher oxidation potential, while the electron-rich CB demonstrates greater reduction potential. Consequently, the Z-scheme mechanism facilitates efficient charge separation and significantly boosts the photocatalyst's redox performance [30,31]. For example, in 2013, Yu et al. introduced the concept of a direct Z-scheme photocatalyst to explain the enhanced photocatalytic degradation of formaldehyde (HCHO) observed in the $\text{TiO}_2/\text{g-C}_3\text{N}_4$ composite. Although the structural configuration of a Z-scheme resembles that of a type-II heterojunction, the mechanism of charge carrier migration between the two systems differs significantly [32].

Another approach to optimizing Z-scheme photocatalysts is the development of all-solid-state Z-scheme photocatalyst systems, which have seen significant advancements in recent years. These systems involve two semiconductors that are directly connected or linked through a solid electron mediator, such as metal nanoparticles (e.g., Au, Ag). The

direct contact minimizes energy loss, thereby enhancing charge separation and transfer [31] (Figure 1.2c). The CdS/Au/TiO₂ system, fabricated through a simple photochemical method, represents the first reported example of an all-solid-state Z-scheme photocatalyst. Upon UV irradiation, photoexcited electrons in the CB of TiO₂ migrate to Au and subsequently to the VB of CdS, where they recombine with photogenerated holes in CdS. Meanwhile, the electrons remaining in the CB of CdS and the holes in the VB of TiO₂ retain strong reduction and oxidation capabilities, respectively, resulting in enhanced photocatalytic efficiency [33].

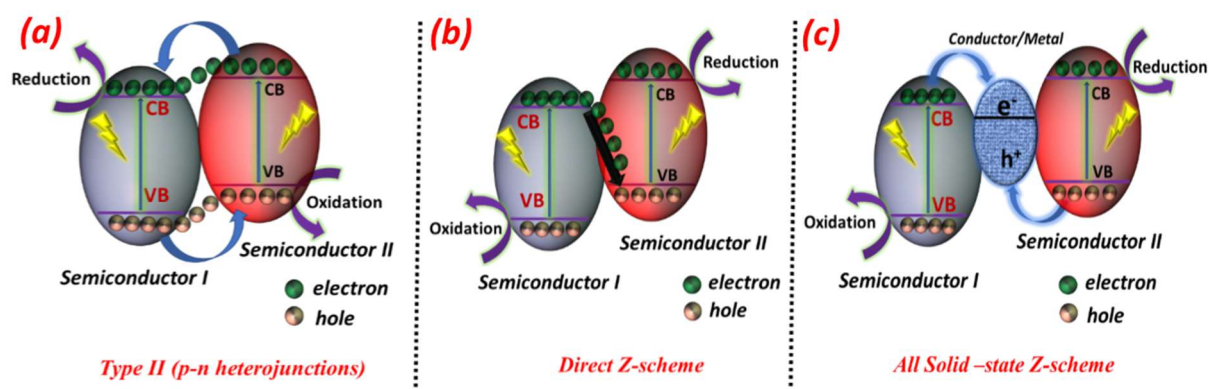


Figure 1.2 Schematic structure of staggered band alignments photocatalysts (a) p-n heterojunction, (b) Direct Z-scheme, (c) All Solid-state Z-scheme.

1.3 Designing of plasmonic metals-semiconductor photocatalyst heterojunctions

Another effective strategy to improve photocatalytic efficiency is the formation of a semiconductor-metal junction, which enhances visible light absorption and suppresses charge carrier recombination. This junction is also known as a Schottky barrier. At the interface between the semiconductor and metal, electrons flow from the material with a higher Fermi level to the one with a lower Fermi level, leading to the alignment of their Fermi energy levels. As a result, a Schottky barrier forms, where the metal accumulates excess negative charges, and the semiconductor accumulates excess positive charges. This

barrier acts as an efficient electron trap, effectively preventing electron-hole recombination. Consequently, the formation of the Schottky barrier enhances photocatalytic performance by facilitating charge separation and extending the lifetime of charge carriers.

Additionally, plasmonic metals such as Au, Ag, and Cu exhibit unique localized surface plasmon resonance (LSPR) properties, which result from the collective oscillation of free electrons when excited by light at specific wavelengths. These LSPR effects significantly enhance photocatalytic efficiency by improving light harvesting through strong absorption and scattering of visible and near-infrared light. Furthermore, the generation of hot electrons facilitates their transfer to the conduction band of a semiconductor or enables their direct participation in the redox reactions of reactants [34].

Recently, many research groups have successfully synthesized various semiconductor–metal heterojunction photocatalysts. For instance, Meng et al. loaded Au NPs onto ZnO using the DP method [35]. This catalyst exhibited better photocatalytic H₂O₂ formation activity than pristine ZnO nanoparticles under UV irradiation. Furthermore, another investigation by Song and co-workers demonstrated that depositing Au NPs onto layered MoS₂ enhanced photocatalytic H₂O₂ production under sunlight irradiation. This improvement was attributed to the superior visible light absorption and suppressed charge recombination facilitated by the Au-MoS₂ junction [36]. In recent years, several other metal-semiconductor heterojunctions have been reported, including Au/g-C₃N₄ [37], Ag/BiVO₄ [38], Pt/WO₃ [39], AuPd-BiVO₄ [40], AuAg/TiO₂ [41], and Pt/KCN [42].

1.4 Synthesis protocol of heterostructure/composite photocatalysts

Based on the above discussion and the advantages of heterostructure or heterojunction photocatalysts, this thesis focuses on the design and development of

different heterostructure photocatalyst systems. The following techniques were employed in the preparation of heterostructure photocatalysts. The detailed synthesis procedures for the designed heterostructure systems are discussed in the respective chapters.

1.4.1 Deposition precipitation method

Deposition-precipitation (DP) is a versatile and facile synthesis method widely used for preparing heterostructure photocatalysts. This technique involves the controlled precipitation of a precursor onto the surface of a support material to form a composite structure. The process begins with the preparation of nanoparticles of the major phase through precipitation, typically using metal salt solutions as precursors. The support material, often in powdered form, is then dispersed in the precursor solution. Adjusting the pH is a crucial step, as an optimal pH ensures selective deposition while preventing bulk precipitation. The reaction is usually conducted at elevated temperatures (50–100°C) to enhance nucleation and growth kinetics. To achieve uniform deposition and promote crystallization, the mixture is allowed to age for a certain period. Afterward, the resulting precipitate is filtered and washed multiple times with deionized water/ethanol to remove any unreacted precursors or byproducts. Finally, the material is dried and often calcined at the required temperature to improve crystallinity, eliminate residual organics, and strengthen adhesion between the deposited phase and the support. For instance, Zhang *et al.* [43] and Li *et al.* [44] used deposition precipitation methodology to prepare surface-decorated heterostructures of $\text{Ag}_3\text{PO}_4/\text{CeO}_2$ and $\text{Ag}_2\text{O}/\text{BiO}(\text{COOH})$, respectively. Similarly, Huang *et al.* [45] fabricated $\text{Cu}_2\text{S}/\text{P25}$ p-n heterojunction nanostructures by the deposition-precipitation technique.

1.4.2 Hydrothermal or solvothermal method

The hydrothermal/solvothermal process is a widely used synthesis method for preparing heterostructure photocatalysts. It involves the crystallization of materials from aqueous or non-aqueous solutions at high temperatures and pressures in a sealed autoclave or reaction vessel. When water is used as the solvent, the process is specifically termed the hydrothermal method, whereas the solvothermal method utilizes organic solvents or a mixture of solvents. A Teflon-lined stainless steel autoclave is commonly used as a reaction vessel for these methods. The elevated temperatures and pressures improve solubility, accelerate reactant diffusion, and enhance reaction kinetics. Additionally, the physicochemical properties of nanomaterials can be precisely tailored by adjusting key experimental parameters, including reaction temperature, duration, and the selection of precursors, solvents, and surfactants. These methods facilitate the production of high-purity nanomaterials with excellent control over their size and shape, making them suitable for various applications. For instance, Zhang et al. employed a solvothermal method to synthesize two-dimensional MoS₂/CdS nanohybrids [46]. Similarly, San et al. utilized a hydrothermal approach to fabricate NiO/ZnO heterojunctions [47].

1.5 General principles of photocatalytic H₂O₂ production

In the preceding discussion, we briefly highlighted the significance of H₂O₂ production through photocatalysis. In this section, we delve into the general mechanism underlying photocatalytic H₂O₂ generation, providing an in-depth exploration of the fundamental processes involved.

Typically, photocatalytic H₂O₂ formation involves oxygen reduction on the CB and the oxidation of water on the VB of the photocatalyst. Figure 1.3 depicts different pathways for photocatalytic H₂O₂ production. Equations 1 to 8 give the reactions involved in potential pathways for photocatalytic production of H₂O₂. Among the oxygen reduction reaction

(ORR) pathways, the direct two-electron O_2 reduction route is thermodynamically more favorable than the four-electron mechanism. Equation 1 describes the direct two-electron oxygen reduction, efficiently producing H_2O_2 . The next equation (2) describes four-electron oxygen reduction resulting in water formation. Equations (3 and 4) summarize the possibilities of the superoxide pathway. If the photocatalyst CB position is negative enough, an electron first reduces O_2 to form $\bullet O_2^-$, which then reacts with protons to form H_2O_2 . Nevertheless, the radicals generated can undergo reactions other than those depicted, making the conversion of superoxide radicals to H_2O_2 non-selective with poor yield.

In the water oxidation half-reaction (WOR), H_2O_2 can be generated via a two-step single-electron pathway or a one-step two-electron pathway. Equations 5 to 8 outline these WOR pathways. In the two-step single-electron WOR pathway, h^+ initially oxidizes H_2O to produce a $\bullet OH$, which then combines with another $\bullet OH$ to yield H_2O_2 (Equations 5 and 6). However, very few photocatalysts possess a VB position that is positive enough ($> +2.73V$ vs NHE) for this process to occur. The four-electron pathway, which produces O_2 , is the most thermodynamically favorable due to its lowest energy level (1.23V) (Equation 8). The generated O_2 then participates in the ORR pathway to produce H_2O_2 . Another possibility is the direct two-electron WOR pathway. Here, the h^+ oxidizes H_2O to H_2O_2 in a one-step, two-electron reaction (Equation 7).

Among these, the $2e^- O_2$ reduction stands out as the most efficient process for directly producing H_2O_2 through photocatalysis (Equation 1). In contrast, the non-selectivity of the superoxide pathway (Equations 3, 4) results in lower H_2O_2 yields. It's worth noting that the $2e^- O_2$ reduction of oxygen has a more positive E^0 value (+0.68V) compared to the requirement for 1-electron superoxide formation. However, the $2e^- O_2$ reduction is hindered by slower kinetics when compared to its 1-electron counterpart.

Key strategies to control the pathway toward H₂O₂:

- Maintain a high dissolved O₂ concentration (e.g., continuous O₂ bubbling).
- Introduce noble metal co-catalysts (e.g., Ag) to selectively promote 2e⁻ and superoxide-mediated reduction steps.
- Operate in slightly acidic to neutral conditions (pH 3–6) to improve H₂O₂ stability.
- Employ sacrificial agents to scavenge photogenerated holes, extending electron lifetime for selective O₂ reduction.
- Use staggered semiconductor heterostructures to spatially separate charge carriers, reduce recombination, and channel electrons toward the 2e⁻ pathway while suppressing the competing 4e⁻ water formation route.

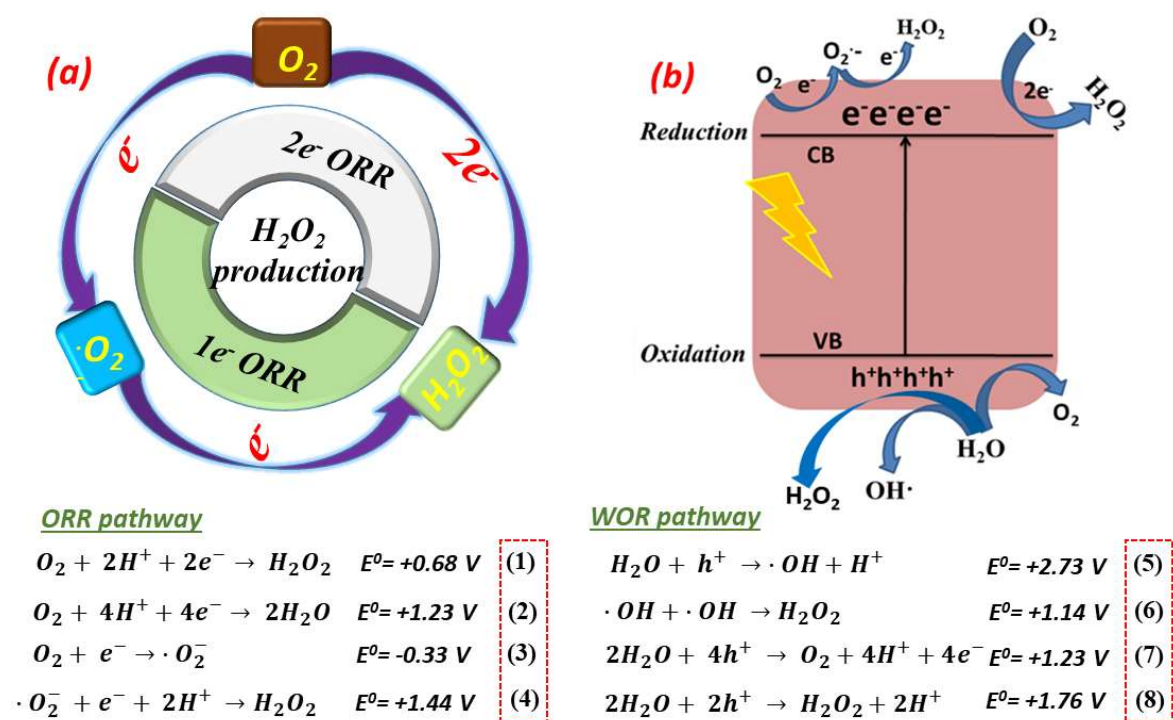


Figure 1.3 (a) Pathway for H₂O₂ production by photocatalysis. (b) General scheme for photocatalytic reaction.

1.6 In situ photo-Fenton degradation of organic pollutants

In the foregoing section, we discussed the photocatalytic reaction pathway for H₂O₂ production. A significant challenge lies in the inability to store or separate the

photocatalytically generated H_2O_2 from the reaction medium. However, this limitation can be turned into an advantage by utilizing the in situ-generated H_2O_2 directly in Fenton or photo-Fenton reactions. The in-situ generation of H_2O_2 eliminates the need for externally supplied H_2O_2 , as required in conventional Fenton or photo-Fenton reactions. This not only mitigates the transportation and storage risks associated with H_2O_2 but also reduces both capital and operational costs. Moreover, the in-situ production and utilization of H_2O_2 on photocatalysts ensures a continuous and controlled supply of the oxidizing agent ($\cdot\text{OH}$). By providing immediate availability of H_2O_2 , this method significantly enhances the effectiveness of environmental applications. Even reactions with low photocatalytic H_2O_2 production activity can still effectively degrade organic pollutants through in situ Fenton processes [48,49]. This is because the H_2O_2 produced, although in small amounts, is rapidly reduced to highly reactive $\cdot\text{OH}$ radicals on the photocatalyst surface, enabling efficient pollutant degradation. It has proven to be an efficient strategy for removing a wide range of pollutants, including organic dyes, phenols, antibiotics, and personal care products (PPCPs). In this process, the in-situ H_2O_2 generated in a photocatalytic stage can be catalyzed into $\cdot\text{OH}$ radicals under light irradiation or photo-Fenton conditions [50,51]. In contrast, direct photocatalytic degradation of pollutants often suffers from low efficiency due to limited charge utilization and competing side reactions, highlighting the superiority of in situ Fenton-based pathways.

Based on the photocatalyst used, in situ Fenton reactions can be classified into three types. The first type involves H_2O_2 -forming photocatalysts that lack an Fe component. In this case, the photo-generated electron on the CB of the photocatalyst performs two roles: in addition to reducing O_2 to form H_2O_2 , it also reduces H_2O_2 to generate $\cdot\text{OH}$ radicals and hydroxide anions (Figure 1.4a) [52]. For instance, Chen et al. developed a benzene and K^+ co-doped $\text{g-C}_3\text{N}_4$ (KBCN) photocatalyst that demonstrated efficient in situ Fenton

degradation of Rhodamine B (RhB) and Congo Red (CR) via photocatalytically generated H_2O_2 . Compared to pristine g- C_3N_4 (PCN), KBCN achieved enhanced H_2O_2 production and Fenton activity due to improved charge separation and accelerated charge transfer. Under visible light irradiation, KBCN degraded 93.3% of RhB and 96.6% of CR within 60 minutes, attributed to the rapid conversion of H_2O_2 into $\cdot\text{OH}$ radicals [53].

The second type involves in situ Fenton reactions catalyzed by Fe-containing photocatalysts, where the H_2O_2 -producing photocatalyst plays a dual role. By incorporating Fe into one component of the photocatalyst, the in situ reduction of photocatalytically generated H_2O_2 to $\cdot\text{OH}$ radicals is effectively facilitated. To enhance this capability, researchers have designed photocatalysts with Fe in their composition, enabling both efficient H_2O_2 production and its subsequent Fenton-based activation (Figure 1.4b). Thus, Zhang et al. developed carbon nanodot-modified FeOCl nanoparticles, where the Cdots acted as active sites to enhance charge carrier separation. This modification shifted the oxygen reduction pathway towards an efficient two-electron reduction for H_2O_2 generation. Additionally, under light irradiation, the photoexcited electrons reduced surface Fe^{3+} to Fe^{2+} , which rapidly activated H_2O_2 , producing a large amount of $\cdot\text{OH}$ radical through a photo-Fenton process [54]. Similarly, Yoon et al. developed Fe-doped g- $\text{C}_3\text{N}_4/\text{WO}_3$ composites and observed that Fe incorporation significantly enhanced $\cdot\text{OH}$ generation compared to undoped g- $\text{C}_3\text{N}_4/\text{WO}_3$. The presence of Fe within the g- C_3N_4 component played a crucial role in the reduction of H_2O_2 to $\cdot\text{OH}$, further supporting the strategy of Fe integration to promote efficient photo-Fenton activity [55].

The third type of reaction system utilizes photocatalysts capable of producing H_2O_2 but lacking Fe. Furthermore, these photocatalysts cannot use photo-excited electrons to reduce H_2O_2 to $\cdot\text{OH}$ radicals (Figure 1.4c). To address this, many researchers have successfully added homogeneous Fe^{2+} salts as Fenton catalysts to degrade organic pollutants. However,

such homogeneous Fenton systems face challenges, including poor recyclability and the generation of sludge. For instance, Wu et al. developed a garland-shaped g-C₃N₄ (GCN) with carbon defects, achieving a photocatalytic H₂O₂ production rate of 507.82 μM g⁻¹h⁻¹. They explored its performance in degrading 2,4-dichlorophenol (2,4-DCP) both with and without Fe²⁺ (from FeSO₄·4H₂O). When Fe²⁺ was added, they termed the process a photocatalytic self-Fenton system (PSFs), specifically referring to the GCN-based version as GCN-PSFs. Compared to bulk g-C₃N₄ (BCN), GCN showed superior photocatalytic degradation of 2,4-DCP even without Fe²⁺. Upon Fe²⁺ addition, degradation efficiency significantly improved, reaching 45.8% for BCN-PSFs and 88.8% for GCN-PSFs [56]. Similarly, Chen and colleagues developed a graphitic carbon-modified g-C₃N₄ photocatalyst by combining graphite with g-C₃N₄, resulting in significantly improved H₂O₂ production compared to pure g-C₃N₄. When FeSO₄·2H₂O was introduced as a Fenton catalyst, the system achieved efficient degradation of RhB, highlighting the synergy between enhanced H₂O₂ generation and Fenton-driven ·OH production [57].

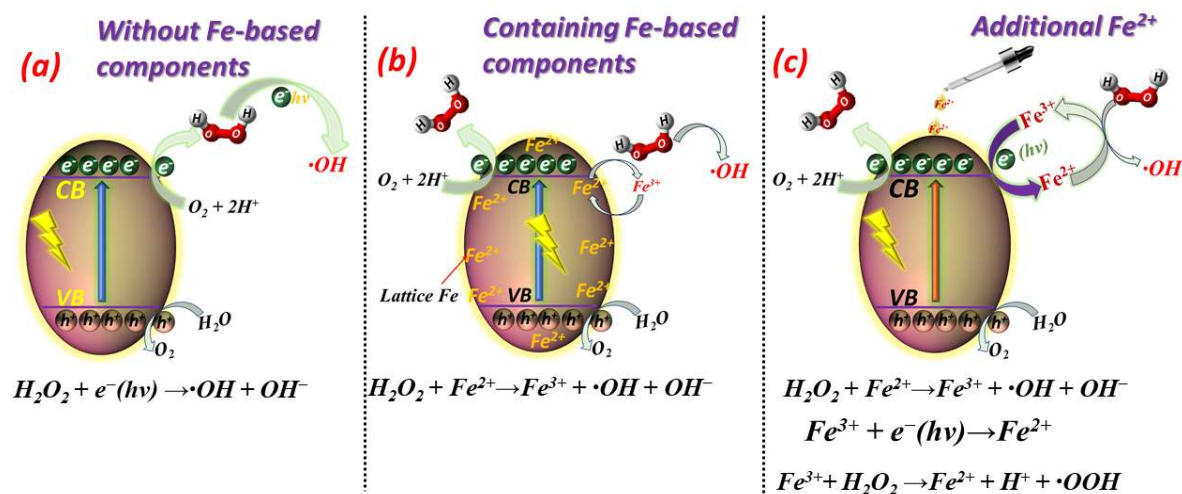


Figure 1.4 Schematic representation of in-situ Fenton reaction (a) without Fe-based component, (b) containing Fe-based components, (c) Addition of homogeneous Fe²⁺ salt in the reaction medium as the Fenton catalysts.

1.7 Research gap

Despite numerous reports on UV- and visible-light-active photocatalysts, many of these systems suffer from either low photocatalytic efficiency or require the use of sacrificial electron donors to enhance H₂O₂ production [58]. Only a limited number of studies have successfully demonstrated photocatalytic H₂O₂ generation using pure water and molecular oxygen as the only reactants [59], revealing a significant research gap in the development of efficient, donor-free photocatalytic systems. To address this challenge, it is essential to consider several key criteria in photocatalyst design. As discussed in the previous section, the construction of heterostructure or composite photocatalysts is a promising strategy to enhance charge separation and facilitate redox reactions. The selection of components for such heterostructures must be done wisely, ensuring that the CB and VB positions are appropriately aligned to drive the desired reduction and oxidation reactions upon visible light irradiation. A typical heterojunction consists of distinct reduction and oxidation components. The CB of the reduction component should efficiently drive O₂ reduction, while the VB of the oxidation component should promote water oxidation. In addition to band alignment and charge separation, surface adsorption of reactants plays a crucial role. The oxidizing and reducing sites must selectively adsorb water and oxygen, respectively, to ensure efficient photocatalytic H₂O₂ generation. However, current research often overlooks the significance of reactant adsorption affinity in heterojunction design. For effective H₂O₂ production, it is imperative to develop photocatalysts that not only exhibit suitable band structures and charge transport characteristics but also possess surface properties conducive to the simultaneous adsorption and activation of O₂ and H₂O. The interplay between these surface adsorption properties and heterojunction design remains a critical yet underexplored factor in advancing donor-free H₂O₂ photocatalysis. To gain deeper insight into this mechanism, this thesis employed large-scale classical molecular

dynamics (MD) simulations to investigate the interactions of oxygen and water molecules with the photocatalyst surface.

In addition, many research groups have primarily focused on photocatalytic H_2O_2 production; however, a significant challenge remains- the difficulty in storing or separating the generated H_2O_2 from the reaction medium. This limitation, however, can be transformed into a strategic advantage by utilizing the in situ-generated H_2O_2 directly in Fenton or photo-Fenton processes [9,60]. Despite this potential, there is still limited research in the literature on in situ Fenton reactions, highlighting an important area for further investigation.

In recent years, heterostructure photocatalysts have been extensively explored for in situ H_2O_2 production to facilitate Fenton degradation of organic pollutants. Reported systems include $BaFe_{12}O_{19}/Ag_3PO_4$ [61], $CdS/rGO/Fe^{2+}$ [62], $Fe_3O_4@ZnO$ [63], $Ag_3PO_4@NiFe_2O_4$ [64], $Fe_2(MoO_4)_3/Ag/Ag_3PO_4$ [65], $Ti_3C_2T_x$ MXene/ CdS [66], $ZnIn_2S_4/FTCN$ [67], $ZnIn_2S_4/TiO_2$ [68], $KPF_6/BiOBr$ [69], MoS_2/FeS_2 [70], and others [54,71,72]. Despite extensive progress in developing heterostructure photocatalysts for in situ H_2O_2 production and Fenton-based degradation, one of the major drawbacks remains their limited stability and reusability over prolonged cycles. Many reported photocatalysts gradually lose activity due to improper interface formation, inefficient charge transfer, and charge accumulation, which accelerate photocorrosion and structural degradation. To overcome these limitations, the design of advanced superparamagnetic and 2D/2D-based heterointerface systems has recently gained attention, although such heterostructure photocatalysts are still underexplored. Another critical challenge hindering large-scale applications is the difficulty of recovery and reuse, particularly for nanoparticle-based

systems that are difficult to separate after each cycle, leading to higher operational costs and potential risks of secondary pollution.

In this context, two complementary strategies have emerged. Superparamagnetic-based heterostructures enable simple and efficient recovery through external magnetic fields, which prevents catalyst loss and allows repeated use without complicated separation procedures. On the other hand, 2D/2D heterostructures provide inherent stability and durability owing to their ultrathin layered architecture, which offers a high surface-to-volume ratio and intimate heterointerface contact. This structural design enhances charge separation, suppresses recombination, and improves resistance to photocorrosion, thereby maintaining high catalytic activity over multiple cycles. Furthermore, the layered morphology facilitates uniform dispersion in aqueous media and enables facile redispersion after use, minimizing catalyst loss during recovery and reuse. Accordingly, this thesis focuses on the design and synthesis of both magnetic-based heterostructure photocatalysts and 2D heterointerface photocatalysts for efficient in situ H_2O_2 production.

1.8 Objectives of the thesis

An extensive literature survey on photocatalyst design for photocatalytic applications highlights that constructing heterostructure photocatalysts can accelerate charge transfer and suppress recombination. The primary objective of this research was to develop advanced heterojunction photocatalysts for efficient photocatalytic H_2O_2 production, with subsequent application in in-situ photo-Fenton degradation of tetracycline.

- (i) The primary objective was to develop a 2D heterointerface $\text{MoS}_2/\text{MnIn}_2\text{S}_4$ photocatalyst, synthesized via a two-step hydrothermal process to enhance solar-driven H_2O_2 production by promoting efficient photo-induced charge separation. The ratio of 2D MoS_2 to MnIn_2S_4 was optimized to achieve the

highest activity. Several control experiments were conducted to investigate the reaction mechanism.

- (ii) Ag/CuWO₄/NiFe₂O₄ heterojunction photocatalyst was prepared to optimize H₂O₂ production under different controlled conditions. The loading of silver onto the CuWO₄/NiFe₂O₄ system was systematically varied to determine the optimum amount for maximum photocatalytic efficiency. The generated H₂O₂ was subsequently utilized for the in situ photo-Fenton degradation of tetracycline. The reaction pathway and mechanism were investigated in detail. Classical molecular dynamics simulations were also performed to gain deeper insights into the reaction mechanism and the role of oxygen adsorption in enhancing photocatalytic performance.
- (iii) This chapter focuses on prepare an Ag/s-(Co₃O₄/NiFe₂O₄) heterojunction photocatalyst for efficient H₂O₂ production. The synthesized heterojunction (Co₃O₄/NiFe₂O₄) was functionalized with starch to enhance its water adsorption properties. Subsequently, the generated H₂O₂ was utilized for in situ photo-Fenton degradation of tetracycline. Additionally, classical molecular dynamics simulations were performed to study the oxygen adsorption properties of the prepared heterojunction photocatalysts.
- (iv) Chapter 6 focuses on the investigation of photocatalytic H₂O₂ production using Ag-loaded, starch-functionalized Fe₃O₄ photocatalysts. This chapter provides an in-depth analysis of the mechanism by which water and oxygen adsorption impact the photocatalytic activity for H₂O₂ production. The proposed mechanism is substantiated through a combination of experimental results and molecular dynamics simulations, offering a comprehensive understanding of the adsorption phenomena and their role in enhancing photocatalytic efficiency.

- (v) In continuation of the above study, this chapter presents the development of a novel heterostructure photocatalyst composed of Ag nanostructures loaded onto starch-stabilized Fe₃O₄/AgI, synthesized via a stepwise co-precipitation method. To enhance the photocatalytic performance, AgI was introduced as a reduction component by loading it onto the Ag-loaded starch-functionalized Fe₃O₄ photocatalyst. The conductive Ag nanostructures served as a metallic bridge between the starch-stabilized Fe₃O₄ and AgI components, thereby facilitating efficient charge separation and transfer. This strategic configuration significantly improved H₂O₂ production, attributed to the enhanced charge transfer efficiency and reduced interfacial resistance. Notably, the resulting photocatalyst exhibited dual functionality, enabling both in situ dark Fenton and photo-Fenton reactions, which effectively degraded tetracycline under ambient conditions.